LETTERS

Millennial- and orbital-scale changes in the East Asian monsoon over the past 224,000 years

Yongjin Wang[1], Hai Cheng[1,2], R. Lawrence Edwards[2], Xinggong Kong[1], Xiaohua Shao[1], Shitao Chen[1], Jiangyin Wu[1], Xiouyang Jiang[1], Xianfeng Wang[2] & Zhisheng An[3]

High-resolution speleothem records from China have provided insights into the factors that control the strength of the East Asian monsoon[1–4]. Our understanding of these factors remains incomplete, however, owing to gaps in the record of monsoon history over the past two interglacial–glacial cycles. In particular, missing sections have hampered our ability to test ideas about orbital-scale controls on the monsoon[5–7], the causes of millennial-scale events[8,9] and relationships between changes in the monsoon and climate in other regions. Here we present an absolute-dated oxygen isotope record from Sanbao cave, central China, that completes a Chinese-cave-based record of the strength of the East Asian monsoon that covers the past 224,000 years. The record is dominated by 23,000-year-long cycles that are synchronous within dating errors with summer insolation at 65° N (ref. 10), supporting the idea that tropical/subtropical monsoons respond dominantly and directly to changes in Northern Hemisphere summer insolation on orbital timescales[5]. The cycles are punctuated by millennial-scale strong-summer-monsoon events (Chinese interstadials[1]), and the new record allows us to identify the complete series of these events over the past two interglacial–glacial cycles. Their duration decreases and their frequency increases during glacial build-up in both the last and penultimate glacial periods, indicating that ice sheet size affects their character and pacing. The ages of the events are exceptionally well constrained and may thus serve as benchmarks for correlating and calibrating climate records.

The last glacial period is characterized by millennial-scale events, first identified in Greenland, including 25 Greenland interstadials (GIS) during the last interglacial–glacial period[11–13]. We previously identified a number of Chinese interstadial (CIS) events[2,4] (relatively strong summer millennial-scale East Asian monsoon, EAM, events) and correlated them with analogous GIS events. We also identified CIS events from portions of the penultimate glacial period, and established a nomenclature with last glacial period CIS denoted CIS A1, A2, and so on, from youngest to oldest, and those of the penultimate glacial period denoted CIS B1, B2, and so on[1]. Here we present an EAM record from Sanbao cave, together with our previous Hulu records[1,2], and characterize the complete CIS series for the last and penultimate interglacial–glacial cycles, including events not previously identified.

Sanbao cave is in Hubei province, central China, on the northern slope of Mt Shennongjia, near the southern edge of the Chinese loess plateau (110° 26′ E, 31° 40′ N, 1,900 m above sea level). Regional climate is dominated by the EAM, a sub-system of the Asian monsoon (AM) (Supplementary Fig. 1), with a mean annual rainfall of 1,900–2,000 mm and a mean temperature of 8–9 °C. During boreal summer (June to September), warm/humid air from the equatorial Pacific penetrates to the northern slope of Mt Shennongjia, delivering more than 80% of annual precipitation. Twelve stalagmites, collected ~1,500 m from the cave entrance, were dated, with 127 ^{230}Th dates with typical errors in age (2σ) of less than 1% (see Methods, Supplementary Table 1 and Supplementary Fig. 2). The record was established with 3,779 δ^{18}O data (see Methods and Supplementary Table 2) with an average resolution of ~70 yr between 224 and 55 kyr before present (BP) and ~40 yr or better between 19 and 0.5 kyr BP.

Virtually identical fluctuations of δ^{18}O from different stalagmites over contemporaneous growth periods (Fig. 1) provide a robust replication test for equilibrium calcite deposition[14] (Supplementary Fig. 3). Furthermore, the Sanbao δ^{18}O record is broadly similar to Hulu and Dongge records[1–4] for all overlapping time intervals (Supplementary Fig. 4), providing another replication test, and indicating that changes in climate have been similar over broad regions of China. Previous studies showed that shifts in stalagmite δ^{18}O largely reflect changes in δ^{18}O values of meteoric precipitation at Hulu and Dongge caves. These shifts, in turn, relate to changes in summer EAM intensity[1,3]. The similarities among the Sanbao, Hulu and Dongge records indicate that the Sanbao record is also a summer EAM proxy.

The EAM fluctuations recorded at Sanbao and Hulu broadly follow orbitally induced Northern Hemisphere summer insolation[10] (NHSI; Fig. 1) and are punctuated by many millennial-scale strong monsoon events (25 in the last glacial cycle, CIS A1–A25, and 24 in the penultimate glacial cycle, CIS B1–B24, Fig. 2 and Supplementary Fig. 5). We previously correlated most of the CIS A events with GIS events[2,4]. The Sanbao data complete this set of correlations through the full set of 25 GIS[13] and CIS A events, including identification of CIS A21, A22 and A25, and their correlation with analogous GIS events. For the penultimate glacial period, we have identified an additional 9 CIS B events so that the full CIS B sequence includes 24 events (Fig. 2 and Supplementary Fig. 5).

When directly compared to each other, there are some striking similarities in the character of analogous CIS A and CIS B events, particularly the older events, CIS A17–A24 and CIS B17–B24 (Fig. 2). In the penultimate interglacial–glacial cycle, the CIS events between 224 and 160 kyr BP (CIS B24–B12) are, in general, longer in duration (average ~3 kyr) and less frequent (~1 event in 5 kyr on average) in comparison with those between 160 and 130 kyr BP (CIS B15–B1, average duration of ~1.5 kyr and frequency of ~1 event in 2.5 kyr) (Fig. 2 and Supplementary Fig. 5). These relationships are similar to the variations of the CIS in the last interglacial–glacial cycle, with an average duration of ~3 kyr and frequency of ~1 event in 4.5 kyr between 110 and 50 kyr BP, and an average duration of ~2 kyr and frequency of ~1 event in 2.5 kyr between 50 and 10 kyr BP. Time–frequency analysis supports this generalization (Supplementary Fig. 6).

Furthermore, cross-spectral analysis between δ^{18}O records of Sanbao/Hulu and Greenland ice[14] over the past 120 kyr also reveals

[1]College of Geography Science, Nanjing Normal University, Nanjing, Jiangsu 210097, China. [2]Department of Geology and Geophysics, University of Minnesota, Minneapolis, Minnesota 55455, USA. [3]State Key Laboratory of Loess and Quaternary Geology, Institute of Earth Environment, Chinese Academy of Sciences, Xi'an, Shanxi 710054, China.

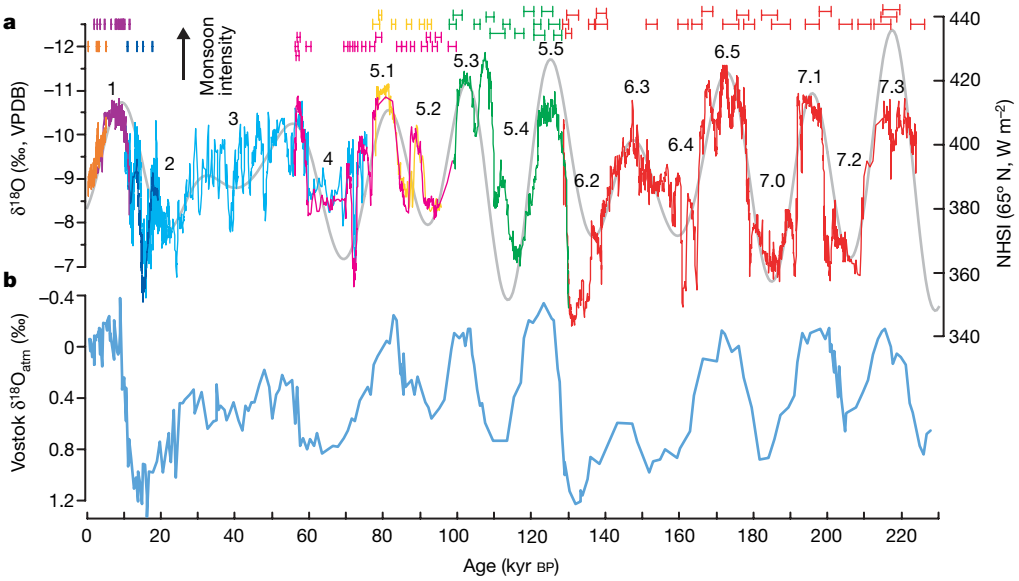

Figure 1 | Comparison of Sanbao/Hulu $\delta^{18}O$ records with NHSI and atmospheric $\delta^{18}O$ record over the past 224 kyr BP. **a**, Time versus Sanbao $\delta^{18}O$ records (red, stalagmite SB11; green, SB23; yellow, SB25-1; pink, SB22; dark blue, SB3; purple, SB10 and orange, SB26) and Hulu cave (blue)[2], and NHSI (Northern Hemisphere summer insolation, 21 July) at 65° N[10] (grey). For comparison, the Hulu $\delta^{18}O$ record is plotted 1.6‰ more negative to account for the higher Hulu values than Sanbao cave (see Supplementary Fig. 4). The ^{230}Th ages and errors (2σ error bars at top) are colour-coded by stalagmites. Numbers indicate the marine isotope stages and substages. **b**, The atmospheric $\delta^{18}O$ record from Vostok ice core, Antarctica[28].

significant common cycles centred at 6.1, 4.7, 4.2, 3.0, 1.6 and 1.2 kyr, similar to North Atlantic ice-rafted debris[15] and/or interstadial cycles[16](Supplementary Fig. 7), supporting the close link between the CIS and GIS. Forcing mechanisms for millennial-scale events have been explained by changing rates of North Atlantic Deep Water formation, resulting in changing heat transport to the North Atlantic[17]. Our data further indicate that (1) the duration and frequency of the millennial-scale events change systematically throughout the course of a glacial period, and (2) that the general nature of these changes is reproducible for the last two glacial periods. These observations suggest a link between ice volume, which could have changed in broadly the same fashion during the last two glacial periods, and the character, duration and pacing of millennial-scale events, consistent with recent simulation results that the mean climate state represented by global ice-volume can pace climatic events[8,9]. Therefore, ice volume, affecting ice dynamics, probably with feedbacks affecting atmospheric and oceanic circulation, may have a significant influence on GIS and CIS events.

The Sanbao/Hulu $\delta^{18}O$ records are characterized by a broadly sinusoidal pattern with a ~23 kyr cycle throughout (Supplementary

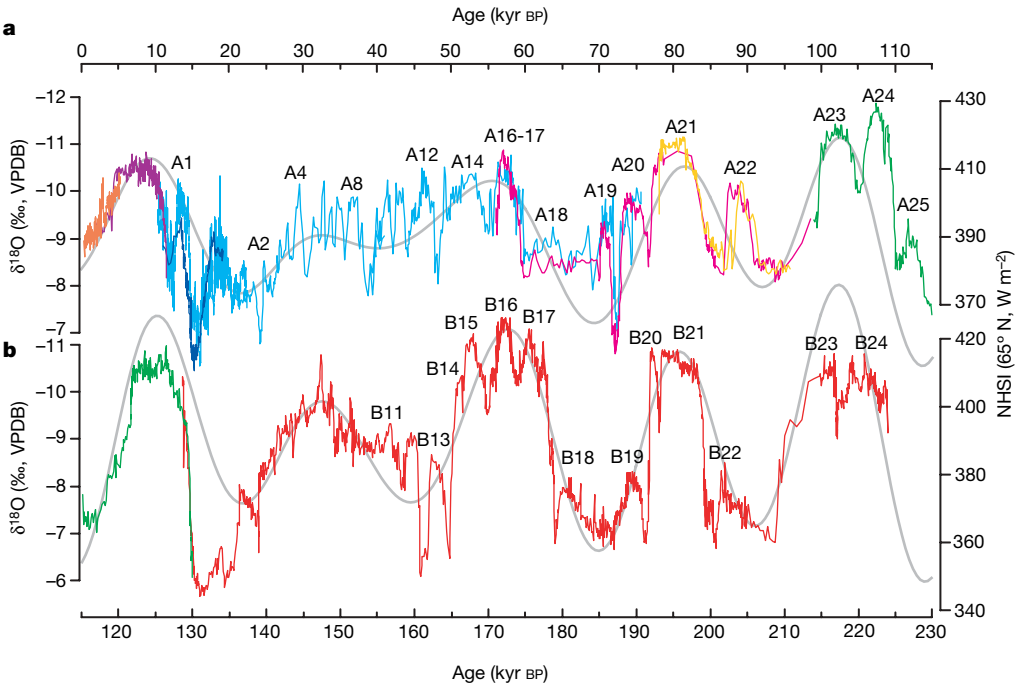

Figure 2 | Comparison of millennial-scale oscillations of the AM between the last and penultimate interglacial-glacial cycles. **a**, Last cycle; **b**, penultimate cycle. The same colours as in Fig. 1 are used to denote samples. Numbers indicate Chinese interstadials[1] (A25 to A1 in the last interglacial–glacial cycle and B24 to B1 in the penultimate interglacial–glacial cycle). See detailed plots of Hulu CIS A1–A13 and B1–B10 in refs 1 and 2. The summer (21 July) insolation at 65° N[10] (grey curves) is also plotted for comparison.

Figs 8 and 9), closely following precession-dominated NHSI (for example, 21 July) changes at 65° N[10] (Fig. 1). This strongly suggests that EAM orbital changes respond approximately linearly to orbital forcing. Spectral analysis ($r = 0.70$, $n = 3{,}206$) further shows no significant phase difference between 21 July insolation and the average EAM signal (lags of the EAM by 0.77 ± 0.45 kyr coherently at 23 kyr cyclicity or $12° \pm 7°$, with 30° equivalent to one month phase shift) (Supplementary Fig. 9).

At higher frequency, millennial-scale events (including CIS events and 'Mystery Intervals' before EAM Terminations I and II[1]) are superimposed on orbital-scale EAM variations. Depending on the relative timing of the millennial-scale and orbital-scale variations, the superposition may result in the appearance of a monsoon lead or lag relative to insolation. The EAM Termination II, dated at 129 ± 1 kyr BP here and in the Hulu and Dongge records[1,3], occurs after the initial rise in insolation by 4–6 kyr. This lag probably results from the occurrence of Heinrich event H11 (correlated to the Weak Monsoon Interval[1]) and its effect on the monsoon during the initial portion of the insolation rise. Similarly, the EAM lead relative to insolation at around 110 to 115 kyr BP might be explained by CIS A24 and A25 (Fig. 1). In addition, the monsoon shift associated with the last deglaciation begins at about 21 kyr BP, synchronous with the insolation minimum. The shift to interglacial values was punctuated by monsoon shifts that correlate with the Oldest Dryas (Heinrich event 1) and the Younger Dryas, explaining apparent EAM lags[7] of ~2 kyr relative to insolation during the last deglaciation (Fig. 2).

Given the observations above, our EAM records confirm an earlier hypothesis[5] that tropical monsoons vary dominantly and directly in response to the changes in Northern Hemisphere summer solar radiation on orbital scales. Onset of the modern Asian summer monsoon occurs in late May–early June as seasonal insolation change results in the reversal of the temperature gradient between land and ocean. Overall EAM rainfall reaches its peak in July in China. Analogous to the seasonal change of the modern EAM, our data show that NHSI change also drives the EAM on orbital scales through similar changes in the temperature gradient between land and ocean[1]. This contrasts with an idea that ties the AM precession cycle to latent heat transfer from the Southern Hemisphere, on the basis of a lag of the AM (as inferred from sediment cores from the Indian[18] and Pacific Oceans[19]) of $\sim 6 \pm 1$ kyr relative to 21 July insolation. Our data do not support this interpretation, nor do they support the idea of a monsoon lag relative to insolation.

One could plausibly reconcile the data sets if the western part of the AM (recorded in the ocean cores) behaved differently from the eastern portion (recorded in our Chinese cave work). However, this does not seem viable either, as cave studies show synchronous shifts for both regions on millennial[20,21] and orbital scales[3,22]. A second possible explanation[6] suggests that the oceanic monsoon proxies represent a more complicated signal that is not solely representative of the Indian summer monsoon. Here we raise a third possibility. From our correlations[1] between cave-based monsoon records and North Atlantic marine records[23], we know that during Termination II, the marine termination (benthic $\delta^{18}O$) led the abrupt transition into the last interglacial monsoon by several kyr. On the basis of this correlation, the SPECMAP timescale[24] is young by several kyr at Termination II. The idea is also supported by a number of earlier studies[25–27]. As the oceanic monsoon records are tied to the SPECMAP timescale[18], SPECMAP offsets might explain the difference in monsoon-insolation phasing inferred for the ocean and cave records.

The amplitudes of EAM variations follow NHSI in general. However, there are differences in $\delta^{18}O$ amplitudes. The monsoon peaks corresponding to marine isotope stage (MIS) 5.5 and 7.3 are relatively low, and the peak at MIS 6.5 is relatively high (Fig. 1). These differences are similar to precessional features in $\delta^{18}O$ variations of atmospheric O_2 ($\delta^{18}O_{atm}$) recorded in the Vostok ice core[28] (Fig. 1). Using the original timescale for $\delta^{18}O_{atm}$, we calculate a correlation coefficient of $r = 0.58$ ($n = 225$, between the $\delta^{18}O_{atm}$ and our records), a likely minimum value as differential errors in age may well lower the calculated coefficient substantially. This minimum, as well as the visual relationship in Fig. 1, indicate a clear relationship between the EAM and $\delta^{18}O_{atm}$, confirming earlier work linking low-latitude climate and $\delta^{18}O_{atm}$ (refs 26, 29). Today, $\delta^{18}O_{atm}$ differs from that of the ocean, the ultimate source of atmospheric O_2, by ~23.5‰ as a consequence of global photosynthesis (known as the Dole effect[29]). Sea water is the ultimate source of oxygen to the atmosphere, with terrestrial photosynthesis contributing to the isotopic difference through a combination of fractionations associated with evaporation from the ocean, Rayleigh processes in the atmosphere, meteoric precipitation, transpiration and photosynthesis[29]. The ultimate source of oxygen for EAM precipitation is also sea water, with isotopic compositions largely governed by the first three of the above processes.

The likely mechanistic link between changes in the Dole effect and changes in the EAM is changes in the average isotopic composition of terrestrial leaf water, through changes in the isotopic composition of meteoric precipitation and relative humidity, both of which might reasonably correlate with changes in the monsoon. As land photosynthesis contributes on the order of 63% of the oxygen to the atmosphere[29], a shift of only 1.6‰ in leafwater $\delta^{18}O$ would generate a 1‰ shift in $\delta^{18}O_{atm}$ (out of a full amplitude of about 1.6‰ for the whole record). As our monsoon record has an amplitude of about 6‰, changes in the isotopic composition of terrestrial meteoric precipitation (that include and correlate with our observed changes monsoon isotopic composition) could easily account for most of the $\delta^{18}O_{atm}$ shift. Furthermore, as leafwater $\delta^{18}O$ is very sensitive to relative humidity[29], changes in terrestrial relative humidity that correlate with (and include) our observed changes in the monsoon probably contribute to the observed changes in the Dole effect as well. Thus, our data support the idea[26,29] that varying AM intensity plays a key part in changing the Dole effect. This relationship will prove critical in correlating ice-core and monsoon records.

METHODS SUMMARY

All of the stalagmites were cut into halves along the growth axis and the surface polished. Subsamples were drilled along growth axes for ^{230}Th dating at the Minnesota Isotope Laboratory on an inductively coupled plasma mass spectrometer (Thermo-Finnigan ELEMENT) using procedures described in refs 3 and 4. A total of 127 ^{230}Th dates were obtained with typical errors in age (2σ) of less than 1%. Typical uncertainties in age (2σ) are less than 0.5 kyr between 10 and 60 kyr BP, 0.7 kyr between 60 and 130 kyr BP, 1.5 kyr between 130 and 180 kyr BP, and 2.0 kyr between 180 and 224 kyr BP. Linear interpolations between ^{230}Th dates were used to establish chronologies. Among these stalagmites, sample SB11 grew for the longest period of time, from 224 ± 2 to 129.3 ± 0.7 kyr BP. Sample SB11, together with four other stalagmites (see Supplementary Fig. 2 for lithologic profiles and dating positions), were used to reconstruct a monsoon history covering time ranges between 224 and 55 kyr BP and between 19.2 and 0.5 kyr BP, as shown in Fig. 1. Analytical procedures for oxygen isotope ratios ($\delta^{18}O$) are similar to those described in ref. 3 and are further described in Supplementary Table 2. Approximately 100 μg of powder samples were drilled along growth axes of stalagmites and analysed with an on-line, automated carbonate preparation system (Kiel III), linked to a Finnigan MAT-253 gas-source mass spectrometer at the Isotope Laboratory at Nanjing Normal University, China. Standards (NBS19) were run every nine samples to check reproducibility. The standard deviation calculated from the NBS19 measurements is ~0.06‰ for $\delta^{18}O$ values. The subsampling interval is ~1 mm or ~0.5 mm along stalagmite axes, depending on sample growth rates.

Received 6 July 2007; accepted 16 January 2008.

1. Cheng, H. *et al.* A penultimate glacial monsoon record from Hulu Cave and two-phase glacial terminations. *Geology* **34**, 217–220 (2006).
2. Wang, Y. J. *et al.* A high-resolution absolute-dated late Pleistocene monsoon record from Hulu Cave, China. *Science* **294**, 2345–2348 (2001).
3. Yuan, D. X. *et al.* Timing, duration and transition of the last interglacial Asian Monsoon. *Science* **304**, 575–578 (2004).
4. Kelly, M. J. *et al.* High resolution characterization of the Asian Monsoon between 146,000 and 99,000 years B.P. from Dongge Cave and global correlation of events surrounding Termination II. *Palaeogeogr. Palaeoclimatol. Palaeoecol.* **236**, 20–38 (2006).

5. Kutzbach, J. E. Monsoon climate of the Early Holocene: Climate experiment with the Earth's orbital parameters for 9000 years ago. *Science* **214,** 59–61 (1981).
6. Ruddiman, W. F. What is the timing of orbital-scale monsoon changes? *Quat. Sci. Rev.* **25,** 657–658 (2006).
7. Clemens, S. C. & Prell, W. L. The timing of orbital-scale Indian monsoon changes. *Quat. Sci. Rev.* **26,** 275–278 (2007).
8. Sima, A., Paul, A. & Schulz, M. The Younger Dryas — an intrinsic feature of late Pleistocene climate change at millennial timescales. *Earth Planet. Sci. Lett.* **222,** 741–750 (2004).
9. Wang, Z. & Mysak, L. A. Glacial abrupt climate changes and Dansgaard-Oeschger oscillations in a coupled climate model. *Paleoceanography* **21,** PA2001, doi:10.1029/2005PA001238 (2006).
10. Berger, A. L. Long-term variations of caloric insolation resulting from the Earth's orbital elements. *Quat. Res.* **9,** 139–167 (1978).
11. Dansgaard, W. *et al.* Evidence for general instability of past climate from a 250-kyr ice-core record. *Nature* **364,** 218–220 (1993).
12. Meese, D. A. *et al.* The Greenland Ice Sheet Project 2 depth-age scale: Methods and results. *J. Geophys. Res.* **102,** 26411–26423 (1997).
13. North Greenland Ice Core Project members. High-resolution record of Northern Hemisphere climate extending into the last interglacial period. *Nature* **431,** 147–151 (2004).
14. Hendy, C. H. The isotope geochemistry of speleothems – I. The calculation of the effects of different modes of formation on the isotopic composition of speleothems and their applicability as paleoclimatic indicators. *Geochim. Cosmochim. Acta* **35,** 801–824 (1971).
15. Bond, G. *et al.* A pervasive millennial-scale cycle in North Atlantic Holocene and Glacial climates. *Science* **278,** 1257–1266 (1997).
16. Clemens, S. C. Millennial-band climate spectrum resolved and linked to centennial-scale solar cycles. *Quat. Sci. Rev.* **24,** 521–531 (2005).
17. Broecker, W. S. Massive iceberg discharges as triggers for global climate change. *Nature* **372,** 421–424 (1994).
18. Clemens, S. C. & Prell, W. L. A 350,000 year summer-monsoon multi-proxy stack from the Owen ridge, Northern Arabian Sea. *Mar. Geol.* **201,** 35–51 (2003).
19. Morley, J. J. & Heusser, L. E. Role of orbital forcing in East Asian monsoon climates during the last 350 kyr: Evidence from terrestrial and marine climate proxies from core RC14–99. *Paleoceanography* **12,** 483–494 (1997).
20. Sinha, A. *et al.* Variability of Southwest Indian summer monsoon precipitation during the Bølling-Allerød. *Geology* **33,** 813–816 (2005).
21. Cai, Y. J. *et al.* High-resolution absolute-dated Indian Monsoon record between 53 and 36 ka from Xiaobailong Cave, southwestern China. *Geology* **34,** 621–624 (2006).
22. Fleitmann, D. *et al.* Holocene forcing of the Indian Monsoon recorded in a stalagmite from southern Oman. *Science* **300,** 1737–1739 (2003).
23. McManus, J. F., Oppo, D. W. & Cullen, J. L. A 0.5-million-year record of millennial-scale climate variability in the North Atlantic. *Science* **283,** 971–975 (1999).
24. Imbrie, J. *et al.* in *Milankovitch and Climate* Part 1 (eds Berger, A. L., Imbrie, J., Hays, J., Kukla, G. & Saltzman, B.) 269–305 (Riedel, Hingham, 1984).
25. Pisias, N. G., Mix, A. C. & Zahn, R. Nonlinear response in the global climate system: Evidence from benthic oxygen isotopic record in core RC13–110. *Paleoceanography* **5,** 147–160 (1990).
26. Shackleton, N. J. The 100,000 year Ice-Age cycle identified and found to lag temperature, carbon dioxides and orbital eccentricity. *Science* **289,** 1897–1902 (2000).
27. Ruddiman, W. F. Orbital insolation, ice volume, and greenhouse gases. *Quat. Sci. Rev.* **22,** 1597–1629 (2003).
28. Petit, J. R. *et al.* Climate and Atmospheric history of the past 420,000 years from the Vostok ice core, Antarctic. *Nature* **399,** 429–436 (1999).
29. Bender, M., Sowers, T. & Labeyrie, L. The Dole effect and its variations during the last 130,000 years as measured in the Vostok ice core. *Glob. Biogeochem. Cycles* **8,** 363–376 (1994).

Supplementary Information is linked to the online version of the paper at www.nature.com/nature.

Acknowledgements We thank W. S. Broecker and the late G. Comer for their support of our work, and J. E. Kutzbach, W. F. Ruddiman and Y. Wang for their comments on an early version of the manuscript. This work was supported by National Basic Research Program of China, a Gary Comer Science and Education Foundation Grant, and NSF and NSFC grants.

Author Information Reprints and permissions information is available at www.nature.com/reprints. Correspondence and requests for materials should be addressed to Y.W. (yjwang@njnu.edu.cn), or H.C. (cheng021@umn.edu), or R.L.E. (edwar001@umn.edu).